Journal of Marine Systems 88 (2011) 20–33

Contents lists available at ScienceDirect

Journal of Marine Systems

journal homepage: www.elsevier.com/locate/jmarsys

Hydrology and circulation in a coastal area off Marseille: Validation of a nested 3D model with observations

I.L. Pairaud [a,*], J. Gatti [a], N. Bensoussan [c], R. Verney [b], P. Garreau [b]

[a] Institut Francais de Recherche pour l'Exploitation de la Mer, Laboratoire Environnement Ressources Provence Azur Corse, BP 330, 83507, La Seyne sur Mer, France
[b] Institut Francais de Recherche pour l'Exploitation de la Mer, Laboratoire DYNECO-PHYSED, BP 70, 29480 Plouzane, France
[c] UMR 6540 DIMARS, CNRS-Université de la Méditerranée, Centre d'Océanologie de Marseille, France

ARTICLE INFO

Available online 1 March 2011

Keywords:
Coastal ocean
Hydrodynamical model
Oceanic circulation
Gulf of Lions
Marseille

ABSTRACT

A high resolution 3D coastal ocean model has been applied to the forecast of the oceanic circulation off Marseille (from the Rhone River to the Cap Sicié). The realistic numerical simulations were forced by the Rhone River, meteorological fields and by the surrounding general circulation. A lot of observations providing the stratification and currents in the area were acquired at moorings and from vessel cruises during the last decade. In order to validate the nested forecasting system, quantitative comparisons between observations and model results were performed for the years 2007 and 2008. Statistics over long time series of temperature at moorings were computed to show the model skills in capturing the monthly to seasonal variability of the thermal structure. The comparison also demonstrated the model's ability to reproduce the observed features over the shelf, like the warming or cooling of the sea due to upwelling and downwelling events. The model also reproduced an intrusion of the Rhone River plume observed into the southern bay of Marseille during a flood event, inducing a salinity decrease at the Frioul station under westerlies and south-easterlies. Hence, although the wind constrains the coastal circulation, the general circulation is also of great influence, with intrusions of the Northern Current from the south of the domain observed and reproduced by the model in winter, due to the penetration of meanders over the narrow eastern part of the shelf. This process was better reproduced by the nested high resolution model than by the North Western Mediterranean Sea model. The nested model was also found to be more suitable to reproduce the plumes of diluted pollutants emanating from coastal discharges.

© 2011 Elsevier B.V. All rights reserved.

1. Introduction

An essential key for the protection and management of coastal waters is to understand the fate of chemical contaminant inputs from major cities and its impact over the adjacent marine ecosystems. The density of contaminant-generating industries of the city of Marseille is highly representative of large modern Mediterranean cities. Marseille was thus chosen for the development of a numerical tool dedicated to the assessment of the chemical contaminant raw inputs (from city to sea) and exports (from mid-sea to open sea). This tool is developed based on the coupling of a hydrodynamical model, a sediment model, a biological model and a model of chemical contamination. This paper deals with the hydrodynamics' compartment, whose validation constitutes the base for the system.

The city of Marseille is located at the eastern part of the Gulf of Lions (goL), where the circulation is constrained by two dominant winds: north-northwest winds (upwelling favorable winds) and southeast winds (downwelling favorable winds). Near Marseille, north-northwest wind gusts induce upwelling zones off the blue coast and off Cassis, as pointed out by Millot (1990) (Fig. 2 Page 888), where the decrease of temperature can reach more than 5 °C. Modifications of the shelf waters are also attributed to the presence of the Rhone River, which is the most significant source of freshwater in the Mediterranean Sea. The associated discharge is around 1700 $m^3 \cdot s^{-1}$ (annual mean) and represents 90% of the total freshwater input in the goL's continental shelf (Fieux, 1974; Durrieu de Madron et al., 2003), with values reaching 10,000 $m^3 \cdot s^{-1}$ during exceptional floods. Due to the oligotrophic nature of the Mediterranean Sea, the inputs of nutrients and chemical contaminants from the Rhone River can greatly modify the biological productivity, which is of major importance for fishery activity. Several studies were dedicated to the Rhone River plume dynamics, both from observations (Broche et al., 1998; Gatti et al., 2006) and from modeling studies (Estournel et al., 1997, 2001; Arnoux-Chiavassa et al., 2003; Reffray et al., 2004). Under north-northwest winds, the plume extends offshore towards the southwest, whereas it is pushed to the coast west of the river inlet under southeasterlies. Gatti et al. (2006) also showed that under certain conditions (combination of a storm with east winds

* Corresponding author.
E-mail addresses: ivane.pairaud@ifremer.fr (I.L. Pairaud), julie.gatti@ifremer.fr (J. Gatti), bensoussan@ipgp.jussieu.fr (N. Bensoussan), romaric.verney@ifremer.fr (R. Verney), pierre.garreau@ifremer.fr (P. Garreau).

0924-7963/$ – see front matter © 2011 Elsevier B.V. All rights reserved.
doi:10.1016/j.jmarsys.2011.02.010

and the presence of Rhone freshwater at the coast), the plume could extend a few tens of kilometers eastward. The thickness of this freshwater surface layer is a few meters close to the mouth and it can reach several tens of meters in the region of Rhone influence (where salinities are lower than 37.8) after mixing with the surrounding waters by the wind. However, the shelf processes are not independent from those of the open sea and the goL is also influenced by the Northern Current (NC) that flows along the continental slope towards the west (Millot, 1990). Indeed, the NC mesoscale activity favors the shelf-slope exchanges as the NC occasionally intrudes on the shelf (Millot and Wald, 1980; Petrenko, 2003; Gatti, 2008).

The number of studies focusing on the circulation in the bay of Marseille and off Cassis is limited. The first work was reported by Castelbon (1972) based on a few current measurements. Later, Albérola and Millot (2003) focused on the circulation in and off the Cassis bay. The circulation was found to be partly down-wind but also greatly influenced by the presence of the Northern Current which can form meanders that penetrate into the bay, especially in winter. Recently, Pradal and Millet (2006) used observational current and meteorological data in addition to the 3D POM model forced by academic winds in order to evaluate the success of artificial production reefs in the southern bay of Marseille. In particular, Pradal and Millet (2006) studied the influence of the wind over the circulation controlling the transport of larvae. They found that the circulation was highly variable in time and space due to the heterogeneity of the wind forcing, with gyres and local up–downwelling systems depending on the wind direction and intensity.

However, the previous model of Pradal and Millet (2006) was not forced by the general circulation or the Rhone River runoff and the study by Albérola and Millot (2003) was based on a few measurements. In this paper, we thus propose a realistic hydrodynamical modeling of the area extending from the Rhone River to the Cap Sicié using the numerical coastal ocean model MARS3D (Lazure and Dumas, 2008) with a high horizontal resolution (200 m). The validation of this modeling by comparison with observations is a prerequisite before making it operational. The model results are validated on the years 2007 and 2008 by comparisons with in-situ observations of temperature, salinity and currents that were obtained during the ANR project MEDCHANGE, the GEOMASTER Tethys II cruise and the SCOPE08 field survey, and with satellite observations of sea surface temperature and ocean color. The validation is presented through a statistical analysis for the seasonal variations of the stratification and by validating the different processes influencing the circulation on the shelf. In particular, we investigate the characteristics of the following processes: upwellings, intrusions of diluted waters from the Rhone River plume toward the bay of Marseille and intrusions of the NC off Cassis from the south of the domain. The capacity of the mesh refinement to capture more details of the coastal circulation is discussed through the study of NC intrusion. The necessity to use a high resolution nested model for pollutant dispersion studies in coastal waters is illustrated by comparing the plumes emanating from an academic coastal discharge in the modelings.

This paper is organized as follows. The model configuration and the observations are presented in Section 2. In Section 3, we describe the seasonal variability of the stratification for the years 2007–2008 and the validation of the model by comparison with observations. The description of the shelf processes off Marseille is given in Section 4. Section 5 deals with the interest of using a high resolution nested model for coastal pollutant dispersion studies. Finally, the results are summarized in Section 6.

2. Materials and method

2.1. Realistic modeling

2.1.1. The MARS3D model

We use the free surface, three dimensional MARS3D model (3D hydrodynamic Model for Applications at Regional Scale, IFREMER) which has been described in detail by Lazure and Dumas (2008), based on the primitive equations and classical Boussinesq and hydrostatic pressure assumptions. As far as the North Western Mediterranean Sea is concerned, this model has been applied to the study of the oceanic surface circulation (Andre et al., 2005), the NC variability (Andre et al., 2009) and associated cross-shelf exchanges (Rubio et al., 2009). Dufois et al. (2008) also used it to study the potential erosion of sediments by the currents and the waves in the Gulf of Lions. An application of the model to the study of the anchovy larvae migration in the goL was performed by Nicolle et al. (2009).

Spatial discretization was done using a staggered 'C' grid (Arakawa and Lamb, 1977) and vertical sigma-coordinates. For this study, the RHOMA model (see Fig. 1) used 503×240 horizontal grid points with a horizontal resolution of 200 m and 30 sigma layers on the vertical (refining the resolution close to the surface and bottom). A mode splitting technique was built with an iterative and semi-implicit method allowing simultaneous calculation of internal and external modes with the same time step. The external mode is solved with an alternating direction implicit (ADI) scheme (Leendertse, 1970). For the RHOMA modeling, the time step is fixed at 60 s.

Viscosity and diffusivity coefficients related to vertical fluxes of temperature, salinity and momentum are given by the turbulence closure scheme of Gaspar et al. (1990). For the horizontal turbulent diffusion, a Laplacian-type horizontal viscosity coefficient is computed from Smagorinsky's formulation (Smagorinsky, 1963), dependent on local mesh dimensions and velocity gradients. The model uses a Quick scheme with a limiter for heat and salt horizontal advection (a second order implicit centered scheme on the vertical), in combination with a second order Quick scheme (Leonard, 1979) for momentum advection.

2.1.2. Model forcing

The initial and boundary conditions are imposed using a downscaling method (Andre et al., 2005) with two levels of grid nesting. First, the North Western Mediterranean Sea circulation model MENOR was forced by the MFS (Mediterranean Forecasting System) 1/16° regional model (Pinardi et al., 2003) daily outputs of temperature, salinity, current and sea surface elevation spatially and temporally interpolated into the MENOR grid. The MENOR configuration, which uses a horizontal resolution of 1.2 km and 30 vertical layers, has been operational since the beginning of 2005 in the framework of the MOON project (http://www.moon-oceanforecasting.eu). For the years 2007–2008, the MENOR modeling was forced by 3-hourly meteorological outputs from a high-resolution (3 km) MM5 model embedded in the NCEP analysis. The MENOR modeling was validated for the years 2005–2006 in the goL by comparing the main characteristics of the simulated shelf-slope circulation with in situ (Andre et al., 2009) and satellite observations (Andre et al., 2005), and for the years 2001–2008 with satellite observations and drifter trajectories in the goL by Nicolle et al. (2009). Afterward, the RHOMA simulation was performed using the 3-hourly outputs (temperature, salinity, currents and sea surface elevation) from the 2007–2008 MENOR simulation of Nicolle et al. (2009), spatially and temporally interpolated for initialization and forcing at the lateral boundaries, following the method by Andre et al. (2005).

The model is also fed by the average daily river inputs from the Grand-Rhone river, deduced from measurements at the Beaucaire station provided by the Compagnie Nationale du Rhone. The average freshwater input for 2007–2008 is 1450 $m^3 \cdot s^{-1}$, with higher values in winter and during the strong floods in June, November and December 2008, reaching 5000 $m^3 \cdot s^{-1}$ (Fig. 2).

At its upper boundary, the model is forced by atmospheric fluxes (modeled wind field, rain and heat fluxes) from the MM5 model (5th generation PSU/NCAR mesoscale model) every 3 h. This model provides radiative solar and long-wave fluxes, humidity, air temperature at 2 m height and wind at 10 m height on a 3 km grid. The wind stress and the latent and sensible heat fluxes are calculated from the

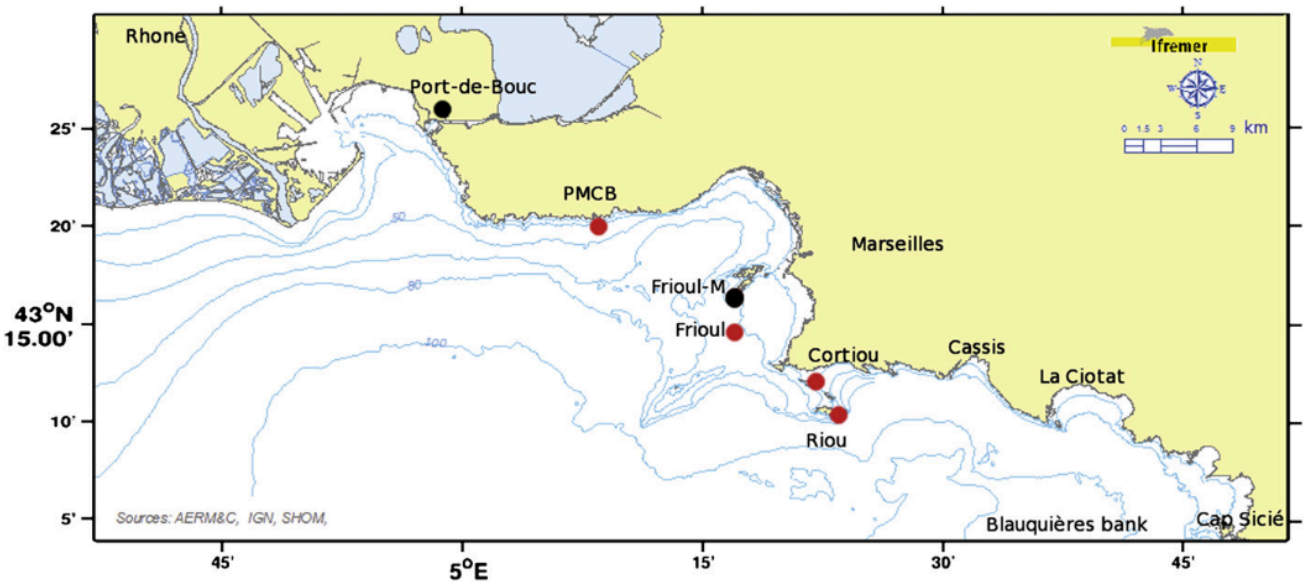


Fig. 1. Map of the RHOMA modeling domain and location of the measurement stations listed in Table 1: PMCB, Frioul, Riou, Cortiou, Port-de-Bouc and Frioul-M. The black dots correspond to meteorological stations, whereas red dots correspond to oceanic stations. Isobaths at 10, 20, 50, 70, 80, 100 and 200 m are drawn.

atmospheric parameters and from the modeled sea surface temperature (SST), using the iterative bulk formulae based on the Monin Obukhov similarity theory (see Geernaert (1990) for details). The choice for a high horizontal resolution atmospheric model (here 3 km) ensures a good representation of orography effects on the wind fields and allows to render the strong variability of atmospheric fluxes. The direction of the dominant wind changes over the RHOMA domain, from north–south at its western part close to the Rhone River mouth (Mistral wind) to east–west at its eastern part close to Cassis. Fig. 3 shows a comparison between the modeled winds and in-situ observations from the meteorological stations Frioul-M and Port-de-Bouc (see Table 1 and Fig. 1 for details). The observations show that the major directions found at the Frioul-M station are 20° westward compared to the directions at Port-de-Bouc (around 300–320° against 320–340° from Fig. 3a and b). The observed winds (Fig. 3a and b) are also more intense at the Frioul-M station, where they reach more than 20 $m^3 \cdot s^{-1}$. The modeled winds (Fig. 3c and d) are in good agreement with the observations at the two locations (Fig. 3a and b), except at the Frioul-M station where the modeled intensities are 30% smaller than the observed ones (most important differences are for summer 2008).

The modeled air temperature above the sea was compared to observed time series at the Frioul-M station. The MM5 temperatures above the sea are close to observations at the Frioul-M station for the period June 2007–December 2008 (not shown). The correlation is of 0.96 over the period (see Section 3.2 for a definition), with a warmer summer in 2008 than in 2007. The bias (B) is of −0.32 °C over the whole period, with a higher value in 2008 than in 2007 (B = −0.5 °C for June–December 2008 and B = −0.26 °C for June–December 2007).

2.2. Observations: hydrological and current data

2.2.1. Fixed stations

Temperature time series collected in the framework of the Medchange project (http://www.medchange.org) and as part of the scientific survey of the 'Parc Marin de la Côte Bleue' (hereafter PMCB) were considered for comparison with RHOMA simulations in the

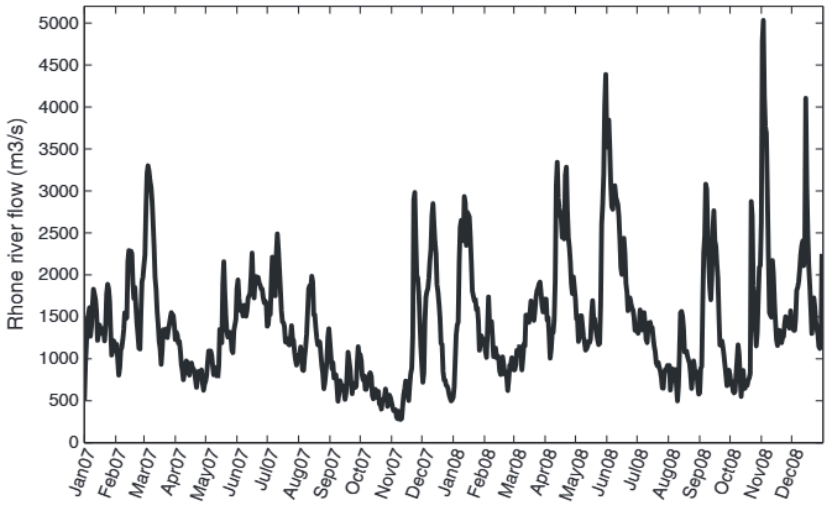


Fig. 2. Rhone River discharge for the years 2007–2008.

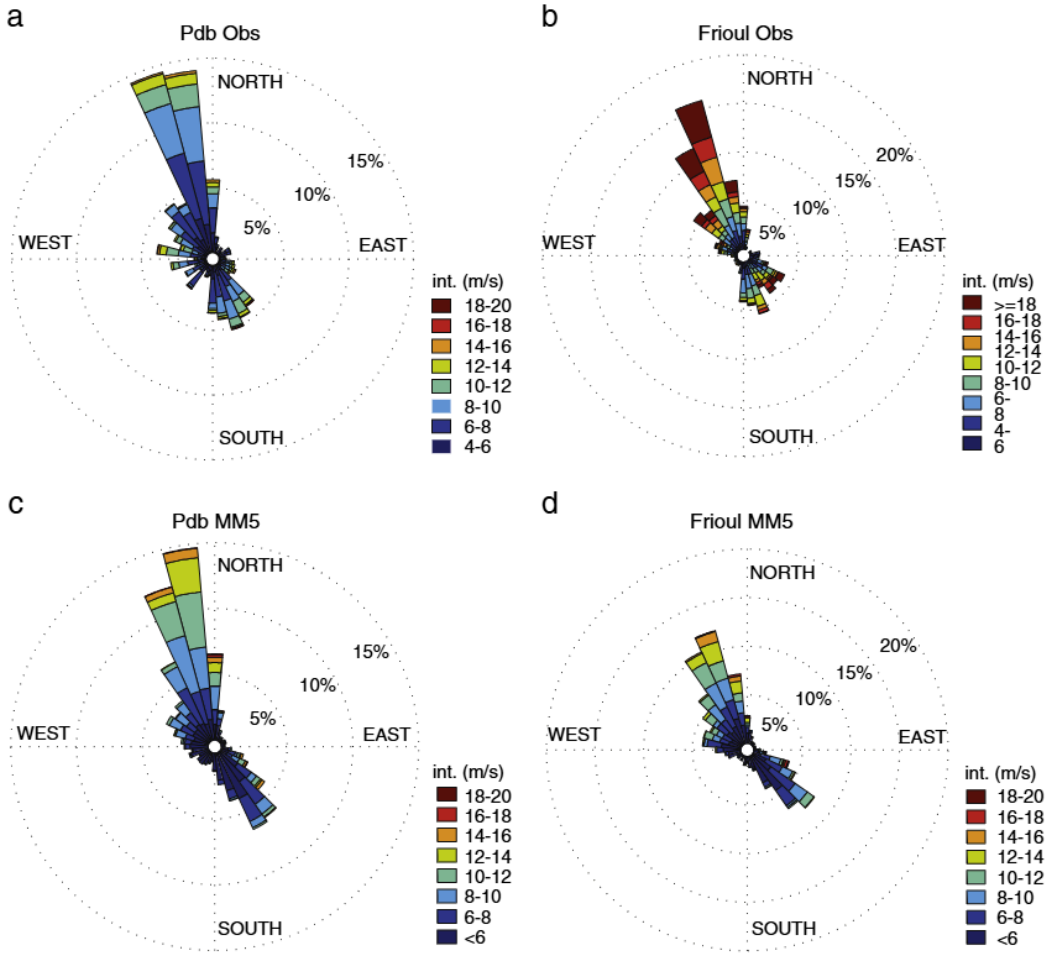


Fig. 3. Comparison of wind roses (intensities and directions at 10 m height) for the wind measured at meteorological stations (a and b) and modeled by MM5 (c and d) for the stations of Port-de-Bouc (a and c) and Frioul-M (b and d).

coastal zone. Temperature was recorded in situ by Stowaway Tidbits autonomous sensors (precision 0.2 °C, resolution 0.15 °C) and recovered annually or semi-annually by divers. The temperature was recorded hourly at 8 depths (5–40 m every 5 m) at Riou Island (Marseille) and every 1 or 2 h at 12, 17 and 23 m depth at the PMCB stations (Carry and Cap Couronne). Deployment sites, periods and depths are shown in Table 1. Measurements at PMCB began in 1997, whereas data at Riou are available since 2003.

In the bay of Marseille, at the south of the Frioul archipelago, time series of temperature and salinity are also available since 1994 (see Table 1 for details). Profiles (0–55 m) are recorded twice a month in the framework of the SOMLIT (Service d'observation en milieu littoral, http://www.domino.u-bordeaux.fr/somlit_national/) network from the INSU (Institut National des Sciences de l'Univers) using a CTD sensor.

Additional occasional measurements were made in the area off Marseille during the SCOPE08 experiment (Vousdoukas et al., 2009). A 1200 kHz RDI ADCP and a CTD were immersed for several months, giving the current profiles and the bottom temperature at the Cortiou station (see Table 1 and Fig. 1).

Table 1
List of the stations where observations of sea current, temperature, salinity and atmospheric data were collected during the years 2007 and 2008. The station's name, dates, latitude (degrees north), longitude (degrees east) are given together with the kind of measured data and the parameters of sampling (P stands for profiles with dz being the vertical resolution, B stands for a measure at the bottom, dt is the temporal resolution and H is the ocean depth). For the wind speed, values are given at an altitude of 10 m above the ground. Rain data are daily accumulated quantity. The atmospheric temperatures are given at an altitude of 2 m above the ground.

Name	Date	Lat N	Lon E	Data type	Parameters
Riou	2007–2008	43.17	5.39	T	P, dz = 5 m, H = −40 m, dt = 1 h
PMCB Carry1	2007–2008	43.32	5.16	T	B, H = −11 m, dt = 1 h
PMCB Carry2	2007–2008	43.32	5.16	T	B, H = −24 m, dt = 1 h
PMCB Couronne	2007–2008	43.32	5.05	T	B, H = −17 m, dt = 1 h
Frioul	2007–2008	43.24	5.29	T/S	P, dz = 0.25 m, H = −57 m, dt = 15 days
Cortiou	10/28/07–12/15/07 10/28/08–12/31/08	43.20	5.38	T/UV	B/P, dz = 1 m, H = −20 m, dt = 0.1 h
Port-de-Bouc	2007–2008	43.42	4.99	UVwind/rain	dt = 1 h/dt = 24 h
Frioul-M	06/01/07–12/31/08	43.28	5.29	UVwind/rain/Tatm	dt = 1 h/dt = 24 h/dt=1 h

2.2.2. Spatio-temporal data

Observations of current, temperature and salinity acquired during the R/V Tethys II cruises have been used by many authors to validate numerical simulations, in particular the dynamics of the NC and its intrusions in the Gulf of Lions (Petrenko, 2003; Andre et al., 2009; Gatti, 2008). The ship is equipped with a hull-mounted ADCP current profiler (RDI broadband 150 kHz). The settings are the same for all the cruises: 60 cells, 4 m depth bins, an ensemble average of 1 min, and bottom tracking when possible. ADCP data analysis is performed with the help of the French INSU (Institut National des Sciences de l'Univers, http://www.saved.dt.insu.cnrs.fr) staff. The first reliable measurement is at a depth of 11 m and the deepest at about 247 m. In addition, a Seabird thermosalinograph connected to an underway pump measures the subsurface temperature and salinity.

In this paper, we chose to consider the GEOMASTER cruise which took place between October 19 and October 21 2007 in the RHOMA area.

Finally, satellite images available at the Nausicaa IFREMER website were used (http://www.ifremer.fr/nausicaa/medit/index.htm). Images of Sea Surface Temperature were extracted from the NAR SST products, based on NOAA AVHRR satellite observations, at a spatial resolution of 2 km. Maps of MODIS ocean color data of Chlorophyll-a processed with the OC5 algorithm were also extracted from the database at a resolution of 1 km.

3. Temporal variability of the stratification for the years 2007–2008: comparison of model results with observations

Observations at the Frioul, Riou and PMCB stations were used to validate the temperature and salinity predicted by the model during the years 2007 and 2008. To evaluate the model's performances, we used time series from models and observations and we computed statistics.

3.1. Time series of temperature and salinity

Comparisons of the temperature and salinity (if measured) time series acquired at the Riou, PMCB and Frioul stations with the simulation outputs were performed every 3 h for the years 2007–2008. Fig. 4 shows a comparison between modeled and observed time series of near surface temperature at the Frioul and Riou stations, and the salinity for the Frioul station. The temperature is at minimum in winter at both stations, with lowest values of about 12.5 °C in the observations, whereas in summer the temperature can reach values of 23 °C (Frioul) to 25 °C (Riou). In winter, the shelf waters tend to be mixed and refreshed under the action of the winds and cold air temperature, and in summer, the heating by the solar and air-sea fluxes favors the stratification of the shelf, which is enhanced in case of weak winds. In summer, the temperature can also be refreshed of 5 to 10 °C in a few hours (see Fig. 4) due to upwellings that appear under NW wind gusts Millot and Wald, 1980 at both locations. As an illustration, in June 2007, the warming of the surface layers at both stations is followed by a rapid refreshment after June 25 under the action of NW wind gusts. The high temporal resolution of the observed temperature time series at the Riou station is particularly well adapted to investigate the differences between the years 2007 and 2008 (Fig. 4c). The in-situ observations show that the near surface waters of winter 2008 were colder than during the winter 2007 of 0.9 °C on average, and that they were warmer in the summer of 0.9 °C on average. Changes in the meteorological conditions (wind and air temperature above the sea) are good candidates to explain those differences. There were more NW wind gusts in summer 2007 than in summer 2008, therefore favoring upwellings and refreshments of the surface waters in summer 2007. In winter, NW winds were strong both in 2007 and 2008 and the air temperature at 2 m above the sea was colder in 2008 than in 2007 (10.33 °C against 10.9 °C on average from January to March for the MM5 model at the Frioul station). This could explain that the water was colder in winter 2008 than in winter 2007.

As a first validation, the MENOR simulation and the nested RHOMA simulation show very similar behaviors at both stations, with nearly superimposed curves of temperature (Fig. 4a and c). In addition, the modeled temperatures fit the observed temperatures in winter and follow the heating tendency in summer, even if the amplitudes of variation are sometimes smaller in the model outputs in this season, especially in 2008. This can be attributed to the underestimation of the wind intensity by the MM5 model at the Frioul-M station (see Fig. 3 and Section 2.1.2), which was more pronounced in 2008, with possible time shifts in the model time series.

Fig. 4b shows the comparison between model and observations of near surface salinity at the Frioul station. The median value of the observed salinity is 38.11, with a minimum of 37 and a maximum of 38.4. However, the deviations from this median value are very small most of the time, with lower values of the salinity in March and June 2007 and in May, June, October and December 2008. An explanation would be the possibility for low salinity waters coming from the Rhone River mouth to reach the Frioul station under particular flow and wind conditions (see Section 4.2 for details).

The modeled salinity looks similar for MENOR and RHOMA simulations, except for low salinity events of June and December 2008. They are in good agreement with the observed salinity most of the time, differences appearing when low salinity waters reach the station. In particular, the presence of low salinity waters is not reproduced for the event of March 2007. The June 2008 low salinity event is better reproduced by the RHOMA simulation than by the MENOR simulation (see Fig. 4b). As the average time step between two points of the time series is 15 days and as we look at a particular location, any small temporal or spatial displacement of the low salinity water patch in the model may result in a poor comparison to observations.

Globally, the temperature seasonal cycle of the upper layers of the sea is therefore well reproduced by the models for the years 2007 and 2008 at the Frioul and Riou stations. The observed time series of salinity is also well reproduced by the model. However, this kind of comparison cannot be shown at every depth and at every station and the next subsection is dedicated to the statistical analysis of the comparisons between the RHOMA model and the observations at the Frioul, Riou and PMCB stations.

3.2. Statistical analysis

Comparisons between modeled and observed Frioul, Riou and PMCB time series were made at all depths. In order to give an overview of the model performance, a box plot (Tukey, 1977) is presented in Fig. 5, showing the mean temperature distribution trends for the observations and for the two configurations MENOR and RHOMA at the Riou station. The models are once again in good agreement with the observations (integrated in time and space). One difference is the largest value for the observations which is 2 °C more than in the models. However, this plot gives global information but it doesn't account for the behaviors of models at different depths.

Statistical metrics chosen to evaluate the model performance at each depth were therefore displayed on summary diagrams. As the two models present large similarities, statistics will be restricted to the comparison of the RHOMA outputs with observations. First, Taylor diagrams (Taylor, 2001) represent the standard deviation (σ) and the correlation (R) statistics, which are respectively given by the formula:

$$\sigma_x = \sqrt{\frac{1}{N-1}\sum_{i=1}^{N}(x_i-\overline{x})^2} \tag{1}$$

$$R = \frac{\frac{1}{N-1}\sum_{i=1}^{N}(m_i-\overline{m})(o_i-\overline{o})}{\sigma_m\sigma_o} \tag{2}$$

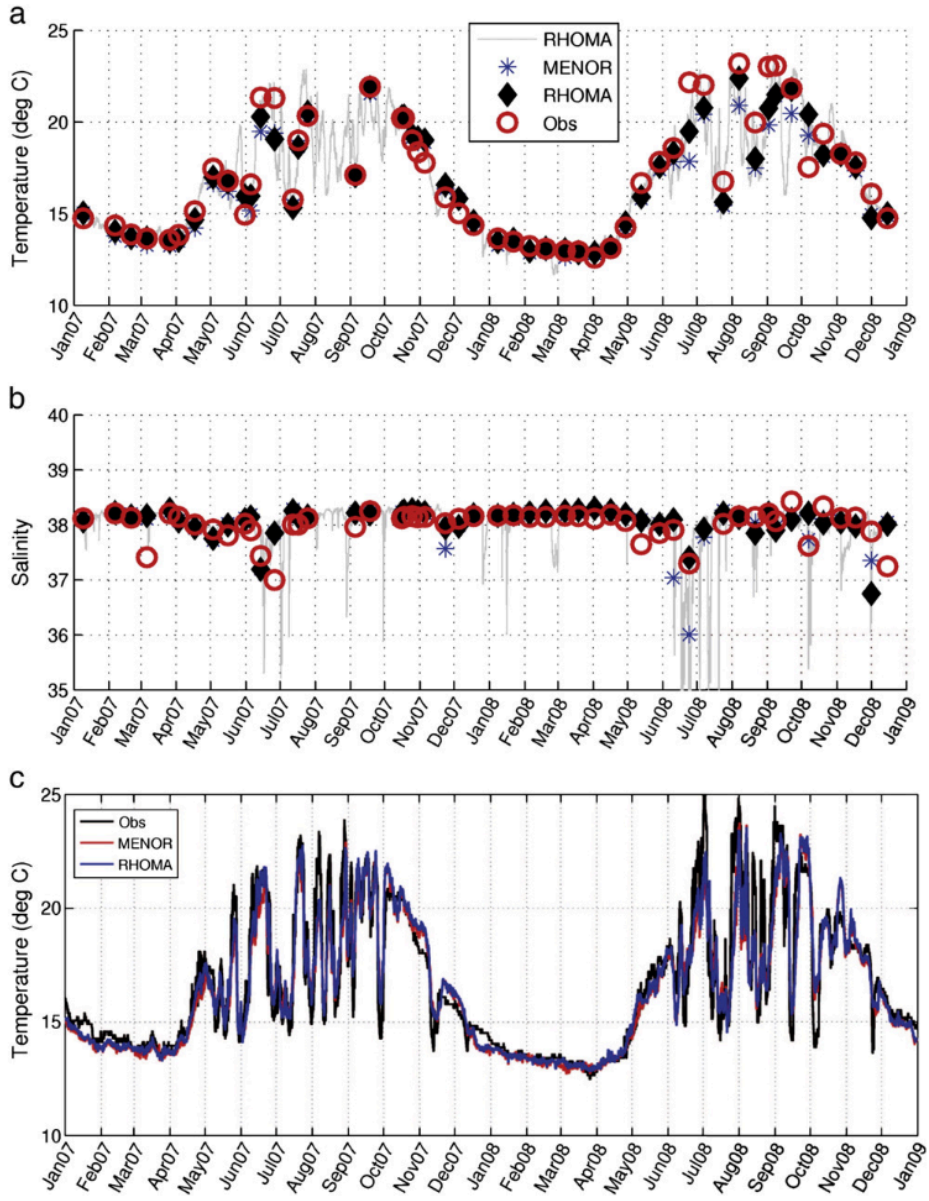


Fig. 4. Comparisons between observations and MENOR and RHOMA model results: Subsurface temperature (a) and salinity (b) at the Frioul station, at a depth of 0.75 m; (c) temperature at the Riou station, at a depth of 5 m.

where x represents the model data (m) or the observed data (o), with $\overline{x} = \frac{1}{N}\sum_{i=1}^{N} x_i$.

The second kind of diagrams is the target diagram of Jolliff et al. (2009) representing the bias (B) and the centered pattern RMS difference (uRMSD) multiplied by the sign of the model and observation standard deviation difference ($\sigma_m - \sigma_o$), with:

$$B = \overline{m} - \overline{o} \tag{3}$$

$$uRMSD = \sqrt{\frac{1}{N}\sum_{i=1}^{N}((m_i - \overline{m}) - (o_i - \overline{o}))^2} \tag{4}$$

Fig. 6 shows the diagrams for the temperature and salinity at the Frioul station (see Table 1 for details).

The three temperature Taylor diagrams confirm that at all locations the standard deviation is higher for the observation than for the model, especially in the 15 first meters of the water column at

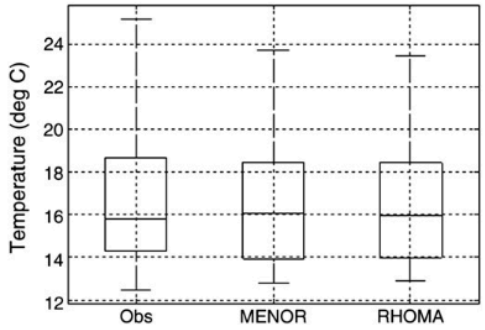


Fig. 5. Box plot representation of temperature distribution at the Riou station for all depths and for years 2007 and 2008. Results are shown for the observations and for the MENOR and RHOMA simulations. The bottom and top of the box are the 25th and 75th percentile (the lower and upper quartiles, respectively), the band near the middle of the box is the 50th percentile (the median), and the ends of the whiskers represent the minimum and maximum values.

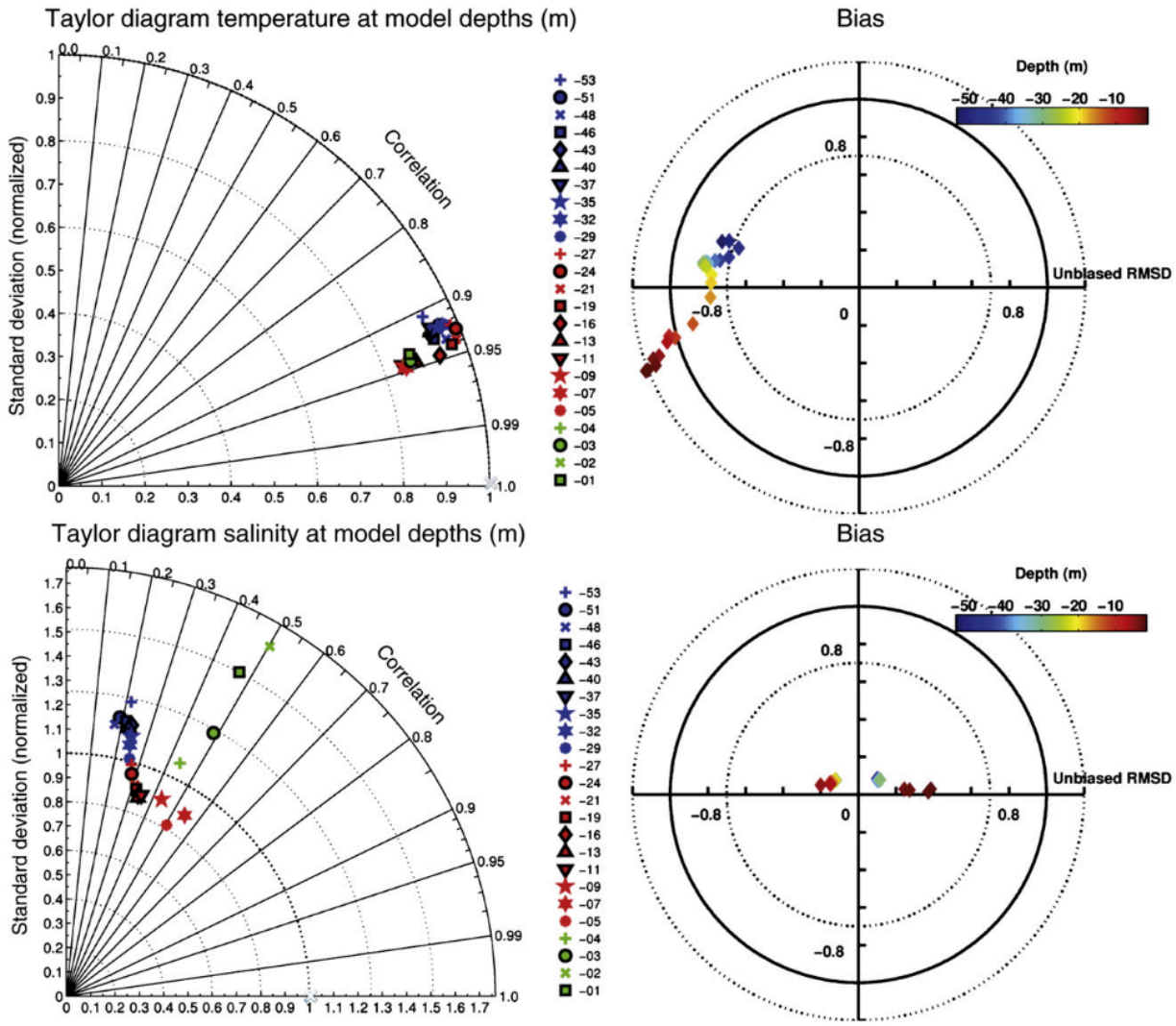


Fig. 6. Model (RHOMA) performance analyses using Taylor diagrams (left) and target diagrams (right) for temperature (top) and salinity (bottom) depending on the depth at the Frioul station. For the Taylor diagrams, the radial distance from the origin is the standard deviation of the modeled temperature or salinity normalized by the standard deviation of the observations. The azimuth angle represents the linear correlation coefficients R between the observations and the modeled temperature or salinity. The distance between each model symbol and the observation (point of coordinates (1,1)) is the uRMSD. A different symbol is used at each depth, colored in green, red and blue (from surface to bottom). For the Target diagrams, the Y-axis corresponds to the bias, the X-axis corresponds to the uRMSD multiplied by the sign of the model and observation standard deviation difference, and the distance from each point to the origin is proportional to the total RMSD. A different color is used at each depth, from red (surface) to blue (bottom).

the Frioul station where they are below 0.9. This low normalized standard deviation for the model is a consequence of the smaller variations in the surface temperature compared to observations previously noted in summer at the Frioul station (see Section 3.1). The correlation coefficients are all higher than 0.9, showing the model's ability to follow the temperature seasonal cycle at all depths. However, those diagrams do not account for the bias and the corresponding target diagrams of Fig. 6 add some valuable information. Bias values are less than 0.6 °C at the Frioul station at all depths, and less than 0.4 °C at the Riou and PMCB stations (diagrams not shown), showing a good agreement between model and observations. At the Frioul station, however, the tendency for the model to underestimate the stratification appears in the bias statistics, with temperature underestimated in the upper levels until 20 m depth (negative bias), whereas the temperature is overestimated in depth (positive bias). Looking at the unbiased RMS differences, they are negative at all stations because the model standard deviation is smaller than the observation standard deviation, as was inferred from the Taylor diagrams. Maxima of absolute values of uRMSD are found at the position of maximum bias, that is for upper levels, where they are not far from 1. This maximum value is linked with the fact that the variability of the temperature around the mean value is not very well reproduced by the model. However, any small model's temperature shift in space or time may induce an important uRMSD, so that this metrics has to be considered with care. Overall, the observed temperature is well reproduced by the model at the Frioul, Riou and PMCB stations.

Fig. 6 also shows the model's skill in reproducing the observed salinity at the Frioul station. Correlations shown by the Taylor diagram are low, all below 0.6, especially in the deepest layers where the correlation reaches 0.2. The salinity is nearly constant in time and departures from the mean value are small in depth. The low correlation values of the upper levels may also result from the differences in the representation of the peaks of low salinity at the Frioul station (see Fig. 4). Some low salinity events are not or not well reproduced by the model. The unbiased RMS differences shown by the target diagram are also at maximum in the upper levels, but the bias is close to zero there. At the deepest level, the uRMSD is small and the bias is maximum but below 0.1. Statistics computed for the salinity at the Frioul station may be interpreted with care. Even if the biases are

relatively low, the Taylor diagram is not well adapted to the validation of salinities (the total correlation is less than 0.5).

This validation of the model showed that particular events could affect the hydrodynamics of the RHOMA area, in particular upwellings under NW wind gusts in stratified conditions and intrusions of diluted (low salinity) waters issued from the Rhone River mouth in the southern bay of Marseille. The next part deals with the evaluation of the model's ability to reproduce those events influencing the shelf circulation of the RHOMA area.

4. Analysis of shelf processes off Marseille

Many large variations of the temperature in the RHOMA area were found to be associated with the influence of the atmospheric forcings (mainly air temperature and wind). We also found an influence of the Rhone River far from its mouth. However, as stated by Albérola and Millot (2003) the general circulation, through intrusions of the NC from the south, constitutes a non negligible forcing of the shelf circulation. In what follows, model outputs and observations are used to study the characteristics of those shelf processes.

4.1. Wind forced upwellings

The spatial variability of upwellings bringing cold water to the surface of the Gulf of Lions has been largely described using observations by Millot (1979; 1990). These upwellings are known to persist several days and to be located on specific areas linked to the shape of the coastline (Millot, 1979). In the RHOMA area, Fig. 2.6 by Millot (1990) shows that those upwellings are likely to occur at three major locations: west of the Rhone, off the blue coast (PMCB station) and off the Calanques (west of Cortiou to Cassis) to Cap Sicié. They are generated under strong NW winds and are particularly noticeable in stratified conditions in summer, when they can induce a decrease of the surface temperature of about 1 °C/h, that means the temperature decreases from 20–25 °C to 13–15 °C (Albérola and Millot, 2003). Indeed, in part 3.1 we saw that the presence of strong NW wind could induce such refreshments in summer, both at the Riou and Frioul stations. Upwelling events of the end of autumn may play a major role in the destratification of the sea, as can be seen from the temperature decrease during and after the events of November 2007 and 2008 (see the temperature time series at the Riou station, Fig. 4c). Among others, the upwelling event of late November 2008 has been observed during the SCOPE08 experiment at Cortiou. Horizontal and vertical velocities were recorded together with the bottom temperature, shown in Fig. 7 between November 21 and November 27. There is a maximum of upward vertical velocity impacting all the water column and reaching 5 $cm \cdot s^{-1}$ on the first hours of November 22 (Fig. 7b). It is accompanied with a rapid decrease of the near bottom temperature of 4.5 °C (from 17.8 °C to 13.3 °C) in about 4–5 h (Fig. 7c), and followed by the appearance of a strong southward velocity in the first 10 m of the water column (Fig. 7a). After 2 days (on November 24), the wind weakens and the temperature increases again.

This upwelling was reproduced by the model but the decrease of temperature (not shown here) was not so important (about 3 °C instead of 4.5 °C), as could be guessed from the upwelling signature on the temperature at the Riou station (Fig. 4c). This could be due to the wind forcing field which is not strong enough, as said before. Fig. 8 rather shows a horizontal view of the upwelling's impacted areas for a strong NW wind blowing over the all domain (Fig. 8a). The surface temperature predicted by the RHOMA modeling (Fig. 8b) is compared to a NOAA-AVHRR SST satellite image (Fig. 8c and d) on November 23, at noon. In the Gulf of Lions, cold surface waters characteristics of upwellings are present close to the coasts from Languedoc to Camargue and off the Blauquières bank and Cassis canyon (see Fig. 8c). Comparison of Fig. 8b and d indicates that the model reproduces the surface signature of the upwelling west of the Rhone and off Cortiou and Cassis, even if there is a bias in the modeled temperature of about 0.5–1 °C in the central part of the RHOMA domain.

4.2. The Rhone river plume: conditions for intrusion in the bay of Marseille

Model and satellite SST maps of Fig. 8 also show the cold signature of the Rhone River plume in November 2008, which is heavily constrained

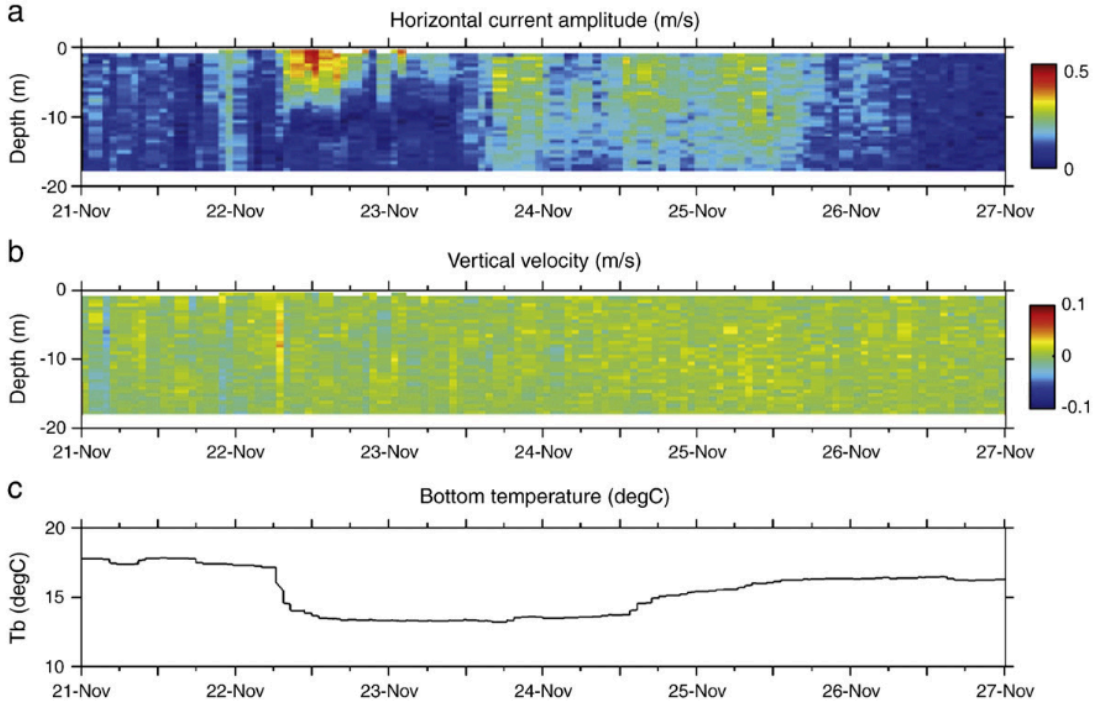


Fig. 7. Observations at the Cortiou station between 21 November 2008 0:00 and 27 November 2008 0:00: (a) amplitude of the horizontal current, (b) vertical velocity and (c) temperature close to the bottom (2 m above seafloor).

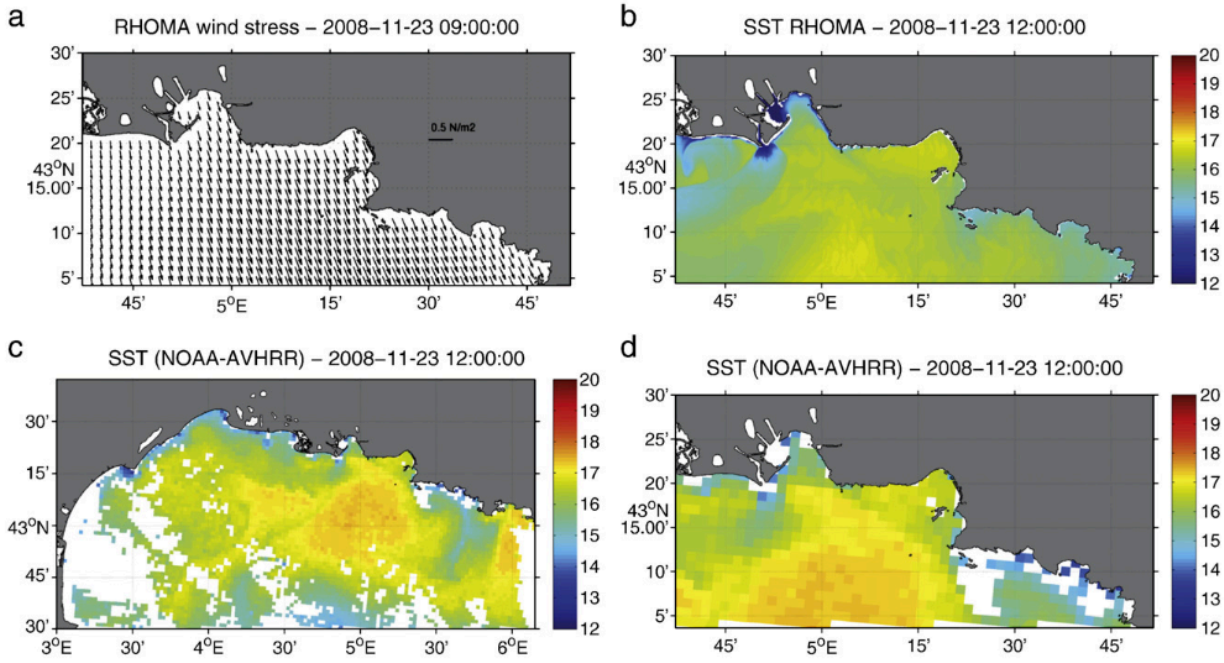


Fig. 8. Wind and sea surface temperature on 23 November 2008: (a) map of RHOMA wind stress at 9:00, (b) map of RHOMA SST ($\sigma = 30$) at 12:00, (c) SST-AVHRR image at 12:00 for the Gulf of Lions and (d) SST-AVHRR image at 12:00 zoomed in the RHOMA area. The white areas on the SST-AVHRR images are due to the presence of clouds.

by the wind, the Coriolis acceleration (which deviates the plume westward) and the surrounding circulation. Under NW wind conditions, the plume extends southwestward on November 23. As described by Reffray et al. (2004), the NW wind induces a separation of the plume from the coast and a spreading of the plume offshore, and the mixing between the surface freshwater and the underlayer marine water is increased offshore due to the wind friction acting on a weakly stratified flow (Xing and Davies, 1999).

For other wind conditions, i.e. after SE winds, low salinity waters thought to result from an eastward extension of the Rhone River plume were observed at the Frioul station on June 24, 2008 (see Section 3.1). Other similar intrusions of desalted waters were recorded at the Frioul station in March 2007, June 2007, June 2008 and December 2008 (Fig. 4b), during flood periods. In June 2008, the Rhone discharge reaches 4500 $m^3 \cdot s^{-1}$ (Fig. 2) and the Rhone plume is likely to spread over a large part of the RHOMA area and to enter the bay of Marseille, as shown by Gatti et al. (2006) for the flood of December 2003.

As the Rhone River is a source of nutrients for the phytoplankton, the Rhone River plume can be associated with an increase of the Chlorophyll-a concentration. As an illustration, Fig. 9 shows an image of MODIS Chl-a concentration over the gulf of Lions for June 23, 2008. In addition to maxima occurring in upwelling areas (close to the coast west of the Rhone River for example), at the eastern part of the gulf the Chl-a maximum accounts for the presence of the Rhone plume. The plume extends over the shelf and some Rhone diluted waters can be found to flow westward at the shelf limit under the action of the general circulation. Fig. 10 shows the RHOMA model salinity together with images of MODIS satellite Chl-a concentration for the period spanning from June 17 to June 23, 2008. Comparisons of the model and satellite data for the three dates: June 17, 19 and 23, show that the extension of the Rhone plume (characterized by a salinity lower than 36.5 on the figure) is well represented by the model compared with the area of maximum Chl-a concentration. In particular, the Rhone River diluted waters are present in the bay of Marseille during several days (Fig. 10a, c and e) and for different wind conditions. On June 17, after 2 days of S winds that pushed the plume toward the coast, NW winds in the western part of the domain tend to push it to flow offshore, whereas at the eastern part of the domain, W winds push the remaining Rhone diluted waters eastward. This results in a plume made of two bulges in Fig. 10a and b. On June 18, under W winds, the large amount of Rhone diluted waters accumulated over the shelf is advected eastward and the presence of desalted waters is reinforced in the bay of Marseille. On June 19 (Fig. 10c and d), SW winds push the desalted waters toward the bay of Marseille again, which is reinforced by the strong W winds of June 20. On June 23 (Fig. 10e and f), after one day of SE winds, the Rhone River diluted waters are still present over the RHOMA area.

In the case of important flood, the Rhone River diluted waters are therefore likely to impact the bay of Marseille for several days, even after the W winds turn into SW or SE winds.

In the next section, another mechanism influencing the shelf circulation and the hydrological characteristics of shelf waters is described, that is the possibility for the NC to intrude the shelf from the south-eastern part of the goL.

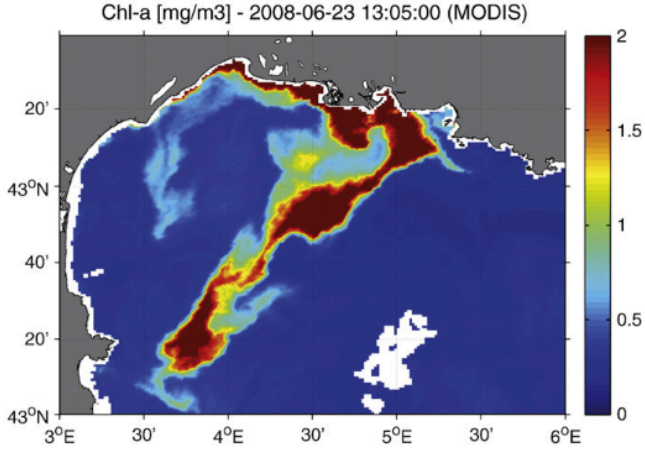


Fig. 9. MODIS Chlorophyll-a image for 23 June 2008 over the Gulf of Lions.

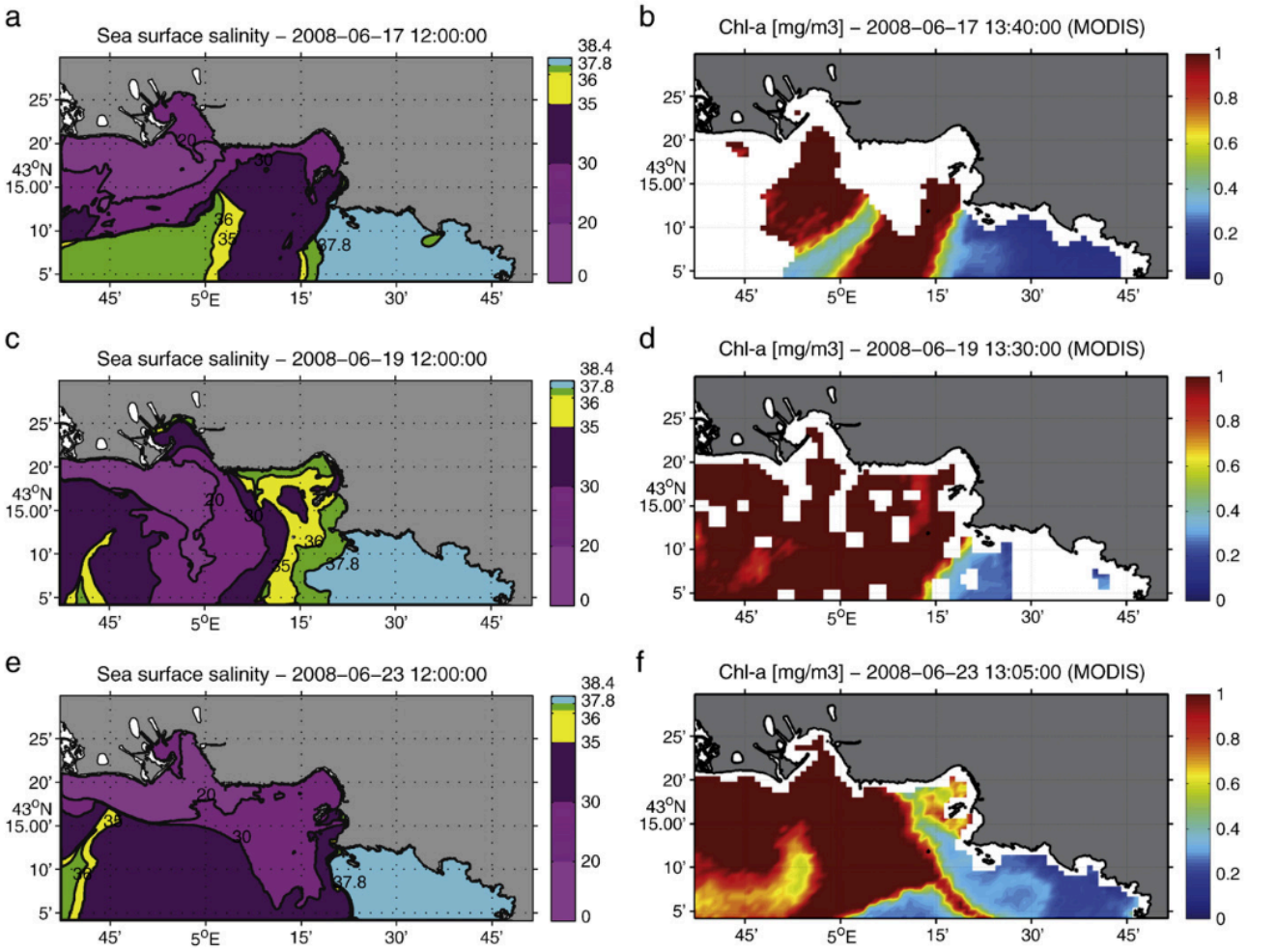


Fig. 10. Evolution of the Rhone River plume from maps of RHOMA modeled surface salinity (left) and maps of MODIS Chlorophyll-a (right) for different dates: (a) and (b): 17 June 2008, (c) and (d): 19 June 2008, (e) and (f): 23 June 2008.

4.3. Northern current intrusion off Marseille

During the GEOMASTER cruise, an intrusion of the NC was detected on October 21, 2007, on the eastern part of the goL's shelf, from at least the Blauquières bank to the Planier canyon (Fig. 11a). The GEOMASTER cruise was not dedicated to the study of the shelf circulation but the speed of the RV Tethys II was low enough to acquire relevant current data with the hull-mounted ADCP.

The RHOMA and MENOR simulated currents were interpolated along the cruise track at each spatio-temporal position of the measured ADCP currents (Fig. 11a). They enhance the intrusion observed in the GEOMASTER data with the northwestern vein of current evolving north of the 200 m depth isobath (defined as the limit of the goL's shelf). The intrusion is underestimated in both models but the RHOMA intrusion is closest to the observed one (depending on the cruise track, from 6% to 57% less intense than the maximum measured currents) with higher intensities of the current than for the MENOR intrusion. On the GEOMASTER shallowest (northern) track over the shelf of Fig. 11a, the RHOMA simulation better represents the intrusion in terms of directions, with currents that are more northward than the currents in the MENOR simulation. Such improvements obtained with the mesh refinement are noticeable at all depths and are due to the better reproduction of the complex bathymetry of the area. Fig. 12 shows a comparison of vertical sections of current along the north–south oriented GEOMASTER track at longitude 5.24 E (middle track perpendicular to the southern boundary of Fig. 11a). The intrusion is confined to the surface layer (above 70 m depth) in the GEOMASTER data (Fig. 12a and b), which is reproduced by the RHOMA simulation (Fig. 12c and d). No hydrologic data is available during the GEOMASTER cruise; nonetheless, in the RHOMA simulation a strong stratification is established at this date (data not shown) and allows the development of this two-layer structure of the water column. In the MENOR simulation (Fig. 12e and f), the intrusion is not confined in the upper layer and higher currents are simulated at depth. The RHOMA simulation thus better reproduces this intrusion. The use of validated models gives us the opportunity to better understand its driving mechanisms than by using only observations that are limited in space and time. The modeled currents at 47 m depth on the entire shelf are presented in Fig. 11b for the RHOMA simulation. They evidence an intrusion by encroaching of the NC (Gatti, 2008). As stated by this author, several processes may induce such an intrusion: the inhomogeneity of Mistral wind, east wind and the NC mesoscale activity. A RHOMA simulation without wind still reproduces the intrusion (data not shown), which dismisses the influence of the local wind. The mesoscale activity of the NC may rather explain the presence of the intrusion. Indeed, the analysis of the circulation in the MENOR simulation reveals that the NC presents meanders (Fig. 11c) which favors the encroaching of the NC and thus its intrusion on the eastern part of the shelf.

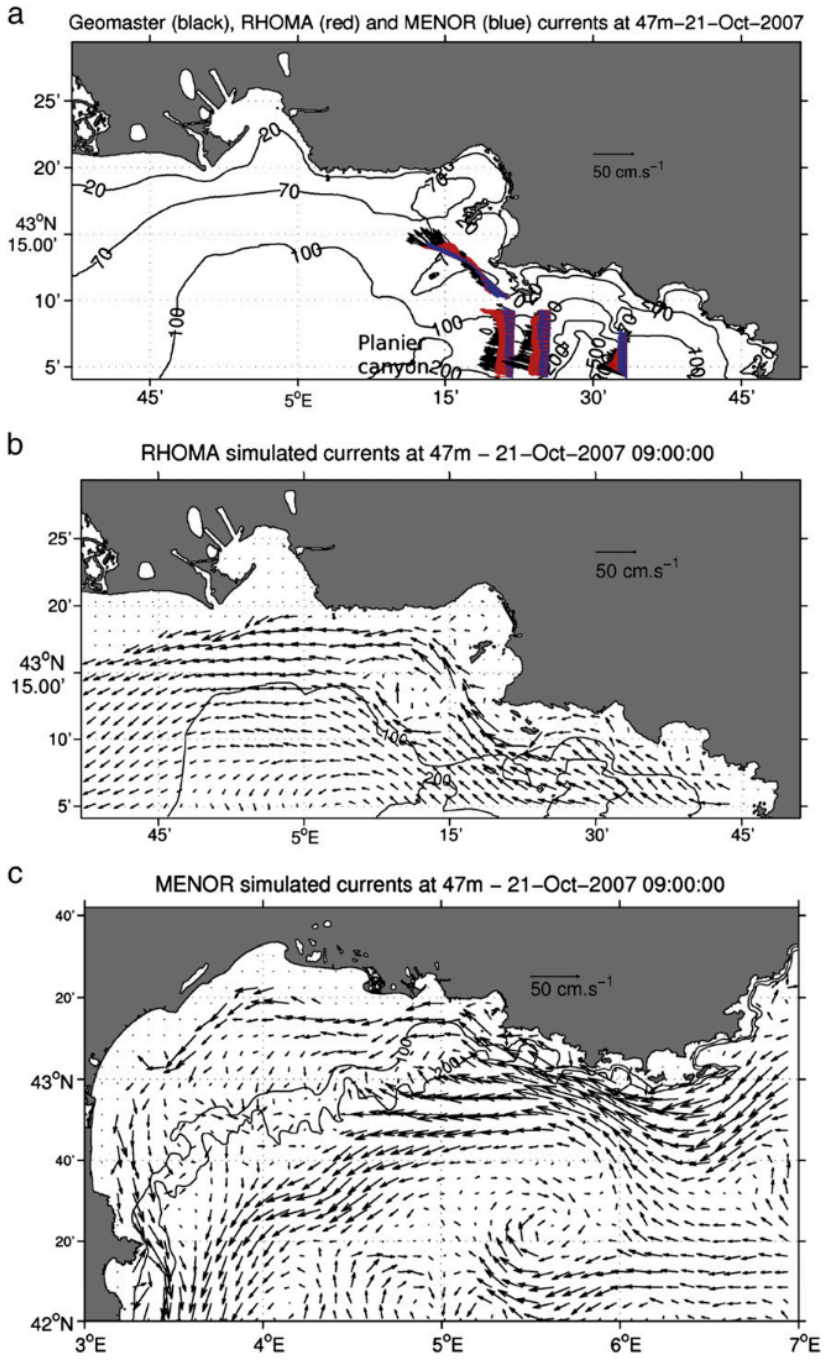


Fig. 11. Maps of horizontal currents in the eastern part of the Gulf of Lions on 21 October 2007: (a) horizontal currents at 47 m depth measured by the hull-mounted ADCP (black), and simulated by RHOMA (red) and MENOR (blue) and interpolated along the GEOMASTER cruise track, (b) horizontal currents simulated by the RHOMA modeling at 47 m depth, (c) horizontal currents simulated by the MENOR modeling at 47 m depth.

5. Interest of using a nested model in coastal areas: academic simulations of a pollutant discharge at the coast

In order to show the interest of using a high resolution nested model in the coastal zone, we performed an academic study of the dilution of a pollutant taken as a passive tracer released at Cortiou (43.21 N, 5.40 E). We considered a flow of 3 $m^3 \cdot s^{-1}$ (average flow from the wastewater treatment plant of Cortiou) containing a dissolved substance whose concentration was set arbitrarily to 100 mg/L. The initial concentration in sea water was set to zero. Variations in the concentration of tracers can be represented by the dilution (ratio of the initial concentration at the outflow to the local concentration). Fig. 13 shows the dilutions obtained for the RHOMA (dx,dy = 200 m, dt = 60 s) and MENOR (dx, dy = 1200 m, dt = 150 s) simulations, for a N wind (a and c) and a SE wind (b and d). In all cases, a rapid high dilution is obtained close to the discharge area. For the northern wind event, the RHOMA dilution zone extends offshore (Fig. 13a), whereas for the south-eastern wind the plume of dilution is pushed toward the coast west of Cortiou (Fig. 13b). In that way, the dilution plume behaves like the Rhone River plume under the influence of such winds. On the contrary, the dilution plumes

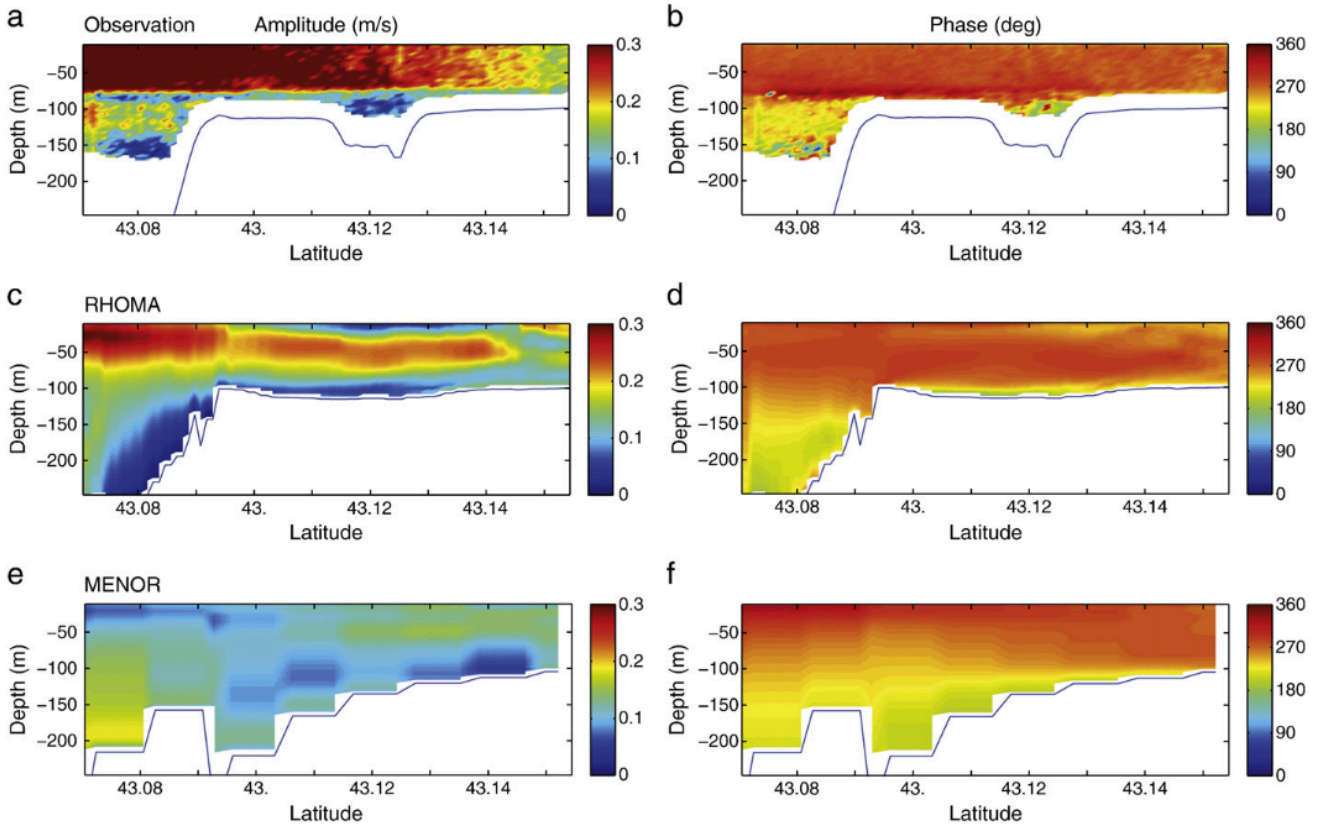


Fig. 12. Vertical section of horizontal currents amplitude (a, c, and e) and phase (b, d, and f) along the 5°24′E GEOMASTER transect (see Fig. 11, middle vertical section) on 21 October 2007, measured by the hull-mounted ADCP (a and b) and modeled by RHOMA (c and d) and MENOR (e and f) and interpolated along the GEOMASTER cruise track. The blue contours on the maps represent the observed bottom depth (a and b) and the models' bathymetry (c, d, e, and f).

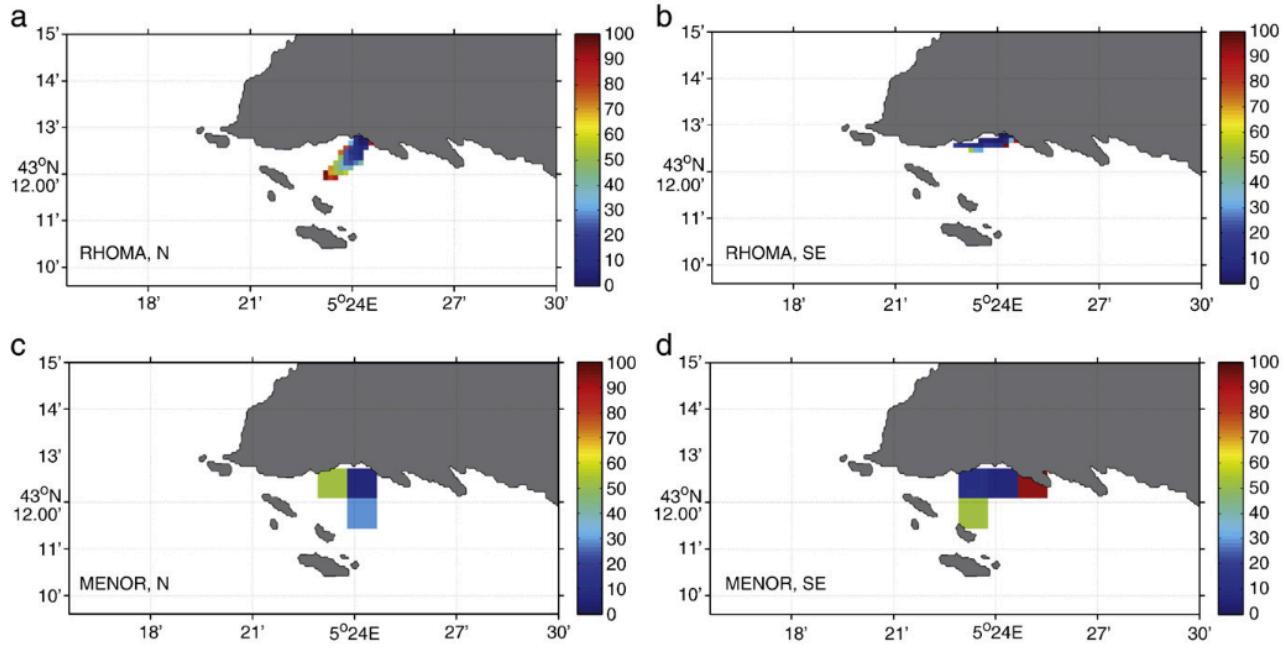


Fig. 13. Maps of dilution of a passive tracer from a discharge at Cortiou under two different winds: north wind (a and c) and south-east wind (b and d) for the RHOMA (a and b) and MENOR (c and d) simulations. Dilutions are restricted to values lower than 100. Results are shown after one month of simulation, for 27 October 2007 at 0:00 (southeast wind) and 15 November 2007 at 18:00 (north wind). No color indicates a dilution larger than 100.

modeled by MENOR (Fig. 13c and d) do not show a clear response to changes in the wind direction. The RHOMA dilution plume is also more refined than the one obtained by MENOR, whose coarser resolution (horizontal mesh grid and time step) doesn't succeed in capturing the dynamics at this coastal scale. From this academic study, the use of a nested high resolution model to simulate pollutant discharge in the coastal zone appears necessary.

6. Summary and conclusion

In this paper, we present a validation of a hydrodynamical model of the eastern part of the Gulf of Lions for the years 2007 and 2008. Both quantitative and process oriented validations were carried out for realistic simulations of the Rhone and Marseille areas. Such a validation strategy is a prerequisite for the set up of an operational model of the area off Marseille, where the good representation of the processes impacting the shelf is of primary importance prior to coupling with other models toward chemical contamination studies.

The quantitative comparison between the modeled temperature or salinity and observations has been made at three different locations (Frioul, Riou and PMCB stations). Statistical representations using Taylor and target diagrams have shown their efficiency in summarizing information from long time series including different depths. From this study, those diagrams would be good candidates for summarizing the information provided by a systematic computation of statistics on temperature and salinity differences between the model outputs and near real-time observations. This is a valuable tool for operational oceanography, which is used for the management and monitoring of coastal waters. The modeled temperature was found to be in good agreement with the observations, with correlations higher than 0.9 and bias lower than 0.6 °C. In particular, the model was able to reproduce the seasonal variability and to a less extent the interannual variability between 2007 and 2008. However, the model underestimates the summer temperature variations associated with upwelling events. The comparison with the observed salinity also illustrated the difficulty to reproduce the extreme events with the model. Some salinity decreases associated to an intrusion of Rhone diluted waters in the southern bay of Marseille are not well reproduced. But the nesting strategy was found to be relevant, as the low salinity event of June 2008 was well reproduced by the RHOMA simulation but not by the larger scale MENOR simulation.

In order to complete the statistics, a second step of process oriented validation has been carried out. It was intended to test the model's ability to reproduce the main processes impacting the oceanic circulation on the shelf. In particular, the model reproduced with accuracy the upwellings of November 2008 that occurred off Cassis and west of the Rhone under NW winds. In agreement with in-situ and satellite observations, the temperature decrease was of 1 °C/h during five hours after the wind induced generation and the event lasted for a few days. As upwellings can bring nutrients to the surface, a good reproduction of the process is crucial to understand the impact of the physics toward biological processes, for example when monitoring the phytoplankton biomass as part of the foodweb in upwelling areas.

We also investigated the conditions for an eastern spreading of the Rhone River plume and its intrusion in the bay of Marseille, focusing on the June 2008 event. The conditions for intrusion in the bay combine a strong river discharge during flood and W winds that push the plume eastward. Originally, the Rhone diluted waters were still present in the bay after several days in our simulations, under SE and SW winds, in agreement with the observations. The influence of the Rhone River on the bay of Marseille was found to be more important than what was thought before. Its impact on biological life and on chemical inputs has to be taken into account when considering the anthropogenic activities that modify our coastal environment near Marseille.

As far as the modeled currents are concerned, owing to the difficulty to compare them to measures acquired at fixed locations, they were validated against observations from a hull-mounted ADCP along transects. As the intrusions of the Northern Current on the eastern part of the Gulf of Lions' shelf constrain the hydrology above the shelf, we chose to validate the currents on this process. Although underestimated, the currents obtained with the model have a good structure (amplitude shifts and directions) for the event of October 2007. The RHOMA modeling was found to better reproduce the intrusion than the MENOR modeling. This comparison also allowed us to precise that it was the NC mesoscale activity which induced the intrusion.

This study illustrates the difficulty to validate the currents computed by a model using measured currents in the area because of their large variability in time and space. However, the use of a nested model showed that we were able to reproduce the major processes. This model could therefore be used in a nesting strategy to force local models of currents for the monitoring of water quality in coastal areas, as asked by the European water framework directive.

The interest of using a high resolution nested model for studying the dilution of a pollutant in the coastal zone was also illustrated by comparing the dilution of passive tracers in the RHOMA and MENOR simulations. As could be expected, the MENOR simulation was not able to capture the dynamics at that scale and the dilution plume was not correctly reproduced by MENOR. At Cortiou, which is the place of the exit of the wastewater treatment plant of Marseille, the dilution was found to be very rapid. This is an important information for the management of coastal discharges and possible pollution events in the area. Also, when focusing on the possible chemical contamination emanating from Cortiou, the stakeholders may be aware that the solid part, that is the understanding of sedimentary processes and the interaction of chemicals with particles, is the key issue. The next step of the modeling exercise is therefore the coupling with the sedimentary processes.

Acknowledgments

This study was funded by the IFREMER project METROC, sustained by the Marseille water agency, the GIRAC project and the PNEC-EC2CO MASSILIA project. The authors gratefully acknowledge J. Garrabou and the Medchange program as well as JG. Harmelin and the 'Parc-Marin de la Côte Bleue' for communication of the Riou and PMCB T time series. We are grateful to the staff of the SOMLIT (Service d'Observation en Milieu Littoral) national network for littoral observations of the INSU (Institut National des Sciences de l'Univers) for providing the data from the SOMLIT-Frioul station. The MM5 model meteorological fields were provided by ACRI. Wind observations at the station of Port-de-Bouc were provided by Meteo-France through collaboration in the GIRAC project. Wind observations at the Frioul-M station were provided by P. Raimbaut from the COM observation service and C. Yohia. We thank Vincent Dutreuil (from DT/INSU) for the ADCP data analysis and the computer team of IFREMER for its support. Many thanks also to Guillaume Charria (who provided matlab programs for plotting the Taylor and target diagrams), Corinne Tomasino, Valerie Garnier, Benedicte Thouvenin, Vincent Dutreuil, Anne Petrenko, Christel Pinazo, Vincent Faure, Francis Gohin and Yves Bidet for their help with the data processing and for their constructive comments. The two anonymous reviewers are thanked for their help in improving the quality of the manuscript.

References

Albérola, C., Millot, C., 2003. Circulation in the french mediterranean coastal zone near Marseilles: the influence of wind and the northern current. Cont. Shelf Res. 23, 587–610.

Andre, G., Garreau, P., Garnier, V., Fraunié, P., 2005. Modelled variability of the sea surface circulation in the north-western Mediterranean Sea and in the Gulf of Lions. Ocean Dyn. 55, 294–308.
Andre, G., Garreau, P., Fraunié, P., 2009. Mesoscale slope current variability in the gulf of Lions. Interpretation of in-situ measurements using a three-dimensional model. Cont. Shelf Res. 29, 407–423.
Arakawa, A., Lamb, V.R., 1977. Computational design of the basic dynamical processes of the UCLA general circulation model. Meth. computational physics 17, 174–267.
Arnoux-Chiavassa, S., Rey, V., Fraunié, P., 2003. Modeling 3D Rhone river plume using a higher order advection scheme. Oceanol. Acta 26, 299–309.
Broche, P., Devenon, J., Forget, P., De Maistre, J., Naudin, J., Cauwet, G., 1998. Experimental study of the Rhone plume, Part I: Physics and dynamics. Oceanol. Acta 21, 725–738.
Castelbon, C., 1972. Etude de la circulation des masses d'eau dans le golfe de Marseille. Tethys 4, 269–312.
Dufois, F., Garreau, P., Le Hir, P., Forget, P., 2008. Wave- and current-induced bottom shear stress distribution in the Gulf of Lions. Cont. Shelf Res. 28, 1920–1934.
Durrieu de Madron, X., Denis, L., Diaz, F., Garcia, N., Guieu, C., Grenz, C., Loye-Pilot, M., Ludwig, W., Moutin, T., Raimbault, P., Ridame, C., 2003. Nutrients and carbon budgets for the gulf of Lion during the Moogli cruises. Oceanol. Acta 26, 421–433.
Estournel, C., Kondrachoff, V., Marsaleix, P., Vehil, R., 1997. The plume of the Rhone: numerical simulation and remote sensing. Cont. Shelf Res. 17, 899–924.
Estournel, C., Broche, P., Marsaleix, P., Devenon, J., Auclair, F., Vehil, R., 2001. The Rhone river plume in unsteady conditions: numerical and experimental results. Estuar. Coast. Shelf Sci. 53, 25–38.
Fieux, M., 1974. Formation d'eau dense sur le plateau continental du golfe du Lion. Colloques Internationaux du CNRS, La formation des eaux océaniques profondes. CNRS, Paris.
Gaspar, P., Gregoris, Y., Lefevre, J.M., 1990. A simple eddy-kinetic-energy model for simulations of the oceanic vertical mixing: tests at station Papa and long-term upper ocean study site. J. Geophys. Res. 95, 16179–16193.
Gatti, J., 2008. Intrusions du courant nord méditerranéen sur la partie est du plateau continental du golfe du Lion. Ph.D. thesis, Université Aix-Marseille II.
Gatti, J., Petrenko, A., Devenon, J., Leredde, Y., Ulses, C., 2006. The Rhone river dilution zone present in the northeastern shelf of the Gulf of Lion in December 2003. Cont. Shelf Res. 26 (15), 1794–1805.
Geernaert, G., 1990. Bulk Parameterizations for the Wind Stress and Heat Fluxes. In: Geernaert, G.L., Plant, W.J. (Eds.), Surface Waves and Fluxes, Kluwer Academic, Dordrecht.
Jolliff, J., Kindle, J., Shulman, I., Penta, B., Friedrichs, M., Helber, R., Arnone, R., 2009. Summary diagrams for coupled hydrodynamic-ecosystem model skill assessment. J. Mar. Syst. 76, 64–82.
Lazure, P., Dumas, F., 2008. An external–internal mode coupling for a 3D hydrodynamical model for applications at regional scale (MARS). Adv. Water Resour. 31, 233–250.
Leendertse, J., 1970. A water-quality simulation model for well-mixed estuaries and coastal seas. Principle of Computation, The Rand Corporation 1 (RM-6230).
Leonard, B., 1979. A stable and accurate convective modeling procedure based on quadratic upstream interpolation. Comp. Meth. Appl. Mech. Eng. 19, 59–98.
Millot, C., 1979. Wind induced upwellings in the Gulf of Lions. Oceanol. Acta 2, 262–274.
Millot, C., 1990. The Gulf of Lions' hydrodynamics. Cont. Shelf Res. 10 (9–11), 885–894.
Millot, C., Wald, L., 1980. The effect of mistral wind on the ligurian current near Provence. Oceanol. Acta 3, 399–894.
Nicolle, A., Garreau, P., Liorzou, B., 2009. Modelling for anchovy recruitment studies in the Gulf of Lions (western Mediterranean Sea). Ocean Dyn. 59 (6), 953–968.
Petrenko, A., 2003. Variability of circulation features in the gulf of Lion NW Mediterranean Sea. Importance of inertial currents. Oceanol. Acta 26, 323–338.
Pinardi, N., Allen, I., Demirov, E., De Mey, P., Korres, G., Lascaratos, A., Le Traon, P.-Y., Maillard, C., Manzella, G., Tziavos, C., 2003. The Mediterranean ocean forecasting system: first phase of implementation (1998–2001). Ann. Geophys. 21, 3–20.
Pradal, M., Millet, B., 2006. Spatial heterogeneity of wind forcing: application to artificial reef functioning influenced by the circulation in the bay of Marseilles. C. R. Biol. 329 (7), 541–550.
Reffray, G., Fraunié, P., Marsaleix, P., 2004. Secondary flows induced by wind forcing in the Rhône region of freshwater influence. Ocean Dyn. 54, 179–196.
Rubio, A., Taillandier, V., Garreau, P., 2009. Reconstruction of the Mediterranean northern current variability and associated cross-shelf transport in the Gulf of Lions from satellite-tracked drifters and model outputs. J. Mar. Syst. 78, 63–78.
Smagorinsky, J., 1963. General circulation experiments with the primitive equation, I. The basic experiment. Mon. Weather Rev. 91, 99–164.
Taylor, K., 2001. Summarizing multiple aspects of model performance in a single diagram. J. Geophys. Res. 106, 7183–7192.
Tukey, J., 1977. Exploratory Data Analysis. Addison-Wesley, Reading, MA.
Vousdoukas, M., Verney, R., Dufois, F., Pinazo, C., Sauzade, D., Meule, S., Cann, P., 2009. Sediment dynamics in the bay of Marseille. Proceedings of Coastal Dynamics 2009, Impacts of human activities on dynamic coastal processes. Tokyo, Japan, pp. 1–15.
Xing, J., Davies, A., 1999. The effect of wind direction and mixing upon the spreading of a buoyant plume in a non-tidal regime. Cont. Shelf Res. 19, 1437–1483.